British Journal of Pharmacology (1998) 125, 771–781
http://www.stockton-press.co.uk/bjp

Pharmacological and molecular characterization of P2X receptors in rat pelvic ganglion neurons

[1,4]Yu Zhong, [1]Philip M. Dunn, [2,3]Zhenghua Xiang, [2]Xuenong Bo & [1]Geoffrey Burnstock

[1]Autonomic Neuroscience Institute, Royal Free Hospital School of Medicine, Rowland Hill Street, London NW3 2PF and [2]Department of Anatomy and Developmental Biology, University College London, Gower Street, London WC1E 6BT

1 The presence and characteristics of P2X receptors on neurons of the rat major pelvic ganglia (MPG) have been studied using whole cell voltage-clamp, *in situ* hybridization and immunohistochemistry.

2 Rapid application of ATP (100 μM) to isolated rat MPG neurons induced moderately large inward currents (0.33–5.3 nA) in 39% of cells (108/277). The response to ATP occurred very rapidly, with an increase in membrane conductance, and desensitized slowly.

3 The concentration-response curve for ATP yielded an EC_{50} of 58.9 μM. The agonist profile was ATP $\geqslant$ 2MeSATP = ATPγS > BzATP, while α,β-MeATP, β,γ-MeATP, UTP and ADP were all inactive at concentrations up to 100 μM.

4 The response to ATP was antagonized by suramin ($pA_2 = 5.6$), reactive blue-2 ($IC_{50} = 0.7$ μM) and pyridoxalphosphate-6-azophenyl-2′,4′-disulphonic acid (PPADS).

5 Lowering the pH from 7.4 to 6.8 produced a marked potentiation (to 339% of control) of the responses to ATP (30 μM), while raising the pH to 8.0 attenuated the responses (to 20% of control). The EC_{50}s for ATP were 28.8, 58.9 and 264 μM at pH 6.8, 7.4 and 8.0, respectively.

6 Co-application of ATP with Zn^{2+} produced a marked enhancement of the responses to ATP, with an EC_{50} of 9.55 μM. In the presence of Zn^{2+} (30 μM), the EC_{50} for ATP was decreased to 4.57 μM.

7 *In situ* hybridization revealed that the P2X receptor transcripts levels in rat MPG neurons are $P2X_2 > P2X_4 > P2X_1$, $P2X_3$, $P2X_5$ and $P2X_6$. The immunohistochemical staining revealed a small number of neurons with strong $P2X_2$ immunoreactivity.

8 In conclusion, our results indicate that there are P2X receptors present on MPG neurons. The pharmacological characteristics of these receptors, the *in situ* hybridization and immunohistochemical evidence are consistent with them being of the $P2X_2$ subtype, or heteromultimers, with $P2X_2$ being the dominant component.

Keywords: P2X receptor; pelvic ganglia; ATP; suramin; reactive blue-2; PPADS; pH; Zn^{2+}; $P2X_{1-6}$ mRNA; polyclonal antisera

Introduction

Adenosine 5′-triphosphate (ATP) acts at cell-surface purinoceptors of two distinct types: P2X receptors which are the ligand-gated cation channels (ionotropic), and the G-protein coupled (metabotropic) P2Y receptors (Abbracchio & Burnstock, 1994). So far, seven P2X receptor subtypes have been cloned, with different amino acid sequences and characteristics, including the agonist profiles, desensitization and sensitivities to antagonists. (Valera *et al*., 1994; Brake *et al*., 1994; Chen *et al*., 1995; Bo *et al*., 1995; Collo *et al*., 1996; Surprenant *et al*., 1996). These P2X receptor subtypes also demonstrate different pH sensitivity (King *et al*., 1996; Stoop *et al*., 1997), and modulation by Zn^{2+} (Wildman *et al*., 1998). The pharmacological profiles of the recombinant P2X receptors do not always match those of the endogenous P2X receptors; thus, it has been suggested that some native P2X receptors are heteromultimeric combinations of P2X subunits (Lewis *et al*., 1995).

The P2X receptors have been studied in a number of neurons, including sensory (Krishtal *et al*., 1983; 1988; Bean, 1990; Robertson *et al*., 1996), sympathetic (Cloues *et al*., 1993), parasympathetic (Fieber & Adams, 1991; Nishimura & Tokimasa, 1996), myenteric (Zhou & Galligan, 1996; Barajas-López *et al*., 1996) and central (Edwards *et al*., 1992) neurons. While the extent of the receptor characterization varies amongst these studies, the P2X receptors demonstrate different properties, indicating the presence of different subtypes on these neurons (Khakh *et al*., 1995).

The neurons providing motor innervation to the bladder and pelvic viscera originate in the pelvic plexus. In most mammals, this is a diffuse and extensive plexus comprised of many widely dispersed ganglia with multiple interconnections. In the rat however, this plexus is much simpler and consists of a pair of major pelvic ganglia (MPG) and four to six small accessory ganglia (Purinton *et al*., 1973). Thus, while atypical, this makes the rat a convenient experimental animal. Anatomically, the MPG are unique amongst autonomic ganglia in that neurons of the MPG are a mixture, receiving both sympathetic and parasympathetic inputs from preganglionic fibres travelling within the hypogastric and the pelvic nerves, respectively (Keast, 1995).

In this study, we sought to determine the presence of P2X receptors on neurons of the rat MPG, to pharmacologically characterize them, and to correlate this with the *in situ* hybridization and immunohistochemical evidence. Furthermore, it enables us to make comparisons with purinoceptors present on other neurons, and with heterologously expressed receptors.

[3] Current address: Department of Histology and Embryology, Second Military Medical University, Shanghai 200433, P.R. China
[4] Author for correspondence.

Methods

Electrophysiology

Isolation of neurons Single neurons of the MPG from 17-day old male Sprague-Dawley rats were enzymatically isolated. The rats were killed by stunning and cervical dislocation, and the MPG, located on the lateral surfaces of the prostate gland (Langworthy, 1965), were rapidly dissected out, and placed in Leibovitz's L-15 medium (Life Technologies, Paisley, U.K.). The ganglia were desheathed and 3–4 deep cuts were made in each before incubation in 4 ml Ca^{2+}/Mg^{2+}-free Hank's Balanced Salt Solution with 10 mM HEPES pH 7 buffer (HBSS) (Life Technologies) containing 1.5 mg ml^{-1} collagenase (Class-II, Worthington Biochemical Corporation, Reading, U.K.) and 6 mg ml^{-1} BSA (Sigma, Poole, U.K.) at 37°C for 40 min. The ganglia were then incubated with 4 ml HBSS containing 1 mg ml^{-1} trypsin (Sigma) at 37°C for 15 min. The solution was replaced with 3 ml growth medium comprising L-15 medium supplemented with 50 ng ml^{-1} nerve growth factor, 10% bovine serum, 2 mg ml^{-1} $NaHCO_3$, 5.5 mg ml^{-1} glucose, 200 IU ml^{-1} penicillin and 200 μg ml^{-1} streptomycin. The ganglia were dissociated into single neurons by gentle trituration with two fire polished glass pipettes of decreasing diameter. The cells were then centrifuged at 900 r.p.m. for 5 min, resuspended in 1 ml growth medium and plated onto 35 mm Petri dishes coated with 10 μg ml^{-1} laminin (Sigma). Cells were maintained at 37°C in a humidified atmosphere containing 5% CO_2 and used between 3 and 48 h after plating.

Whole cell voltage-clamp recording Whole cell voltage-clamp recording was carried out at room temperature using an Axopatch 200B amplifier (Axon Instruments, Foster City, CA, U.S.A.). Membrane potential was held at −70 mV. External solution contained (mM): NaCl 154, KCl 4.7, $MgCl_2$ 1.2, $CaCl_2$ 2.5, HEPES 10, Glucose 5.6, the pH was adjusted to 7.4 using NaOH. Recording electrodes were made from thin-walled glass capillary tubes with fine filament (GC 150TF; Clark Electromedical Instruments, Reading, U.K.) using a two stage puller (PP-830, Narishige, Tokyo, Japan), fire polished, and had resistances of 2–4 MΩ when filled with an internal solution containing (mM): citric acid 56, $MgCl_2$ 3, CsCl 10, NaCl 10, HEPES 40, EGTA 0.1, TEACl 10, and the pH adjusted to 7.2 using CsOH. Data were acquired using pCLAMP software (Axon Instruments). Signals were filtered at 2 kHz.

Drugs were applied in two ways. In some experiments, agonists were applied rapidly by use of a solenoid valve-controlled U-tube system placed very near the cell (Krishtal & Pidoplichko, 1980). In other experiments where antagonists were used, drugs were applied rapidly through a seven-barrel manifold composed of fused glass capillaries inserted into a common outlet tube with a tip diameter of ~200 μm (Dunn *et al*., 1996). Solutions were delivered by gravity flow from independent reservoirs placed above the preparation. Applications of agonists (over 3–5 s) were separated by intervals of 2–3 min, which were sufficient for responses to be reproducible. Antagonists were present for 2–3 min before and during the reapplication of agonists. Schild analysis was performed by conducting a 2+2 assay (Arunlakshana & Schild, 1959). Briefly, two-point ATP log concentration-response lines were obtained under control conditions, then in the presence of various concentrations of the antagonist. The effect of the antagonist was expressed as the dose-ratio, and the pA_2 value determined from the Schild Plot. Each concentration of the antagonist was tested on a different sample of cells.

All responses were normalized to that evoked by ATP (100 μM) in the same cell, unless otherwise stated. All data were expressed as the means ± s.e.mean. The concentration-response data were fitted with the Hill equation: $Y = A/[1 + (K/X)^n]$, where: A is the maximum effect, K is the EC_{50}, and n is the Hill coefficient, using Prism v1.03, GraphPad. In this study, because agonist concentrations exceeding 300 μM were not used, the concentration-response curves did not always reach a maximum. However, the ATP concentration-response curve in the presence of 30 μM Zn^{2+} reached a clear maximum (see Figure 7b). Therefore, unless otherwise stated, agonist concentration-response curves were constrained to this maximum (1.55). Traces were acquired using pCLAMP (Axon Instruments) and plotted using Origin (Microcal, Northampton, MA, U.S.A). Statistical analysis (Student's *t*-test) was performed using Instat.

In situ *hybridization and immunohistochemistry*

Tissue preparation The MPG from 17-day old male Sprague-Dawley rats were dissected as described above. They were rapidly frozen by immersion in −70°C isopentane for 2 min, cut into 10 μm sections in a cryostat, thaw-mounted on poly-L-lycine-coated slides and air-dried. The sections were then fixed in 4% formaldehyde and 0.03% picric acid in 0.1 M phosphate buffer, pH 7.4 for 10 min. After being washed 3 × 5 min in phosphate buffered saline (PBS), they were processed for *in situ* hybridization and immunohistochemistry.

In situ *hybridization* Sense and anti-sense digoxigenin-labelled cRNA probes were synthesised with a DIG-RNA Labelling Kit (Boehringer Mannheim, Lewes, U.K.) using truncated $rP2X_{1-6}$ cDNAs as the templates. The cRNA sequences were corresponding to the nucleotide sequence 1–713 in $rP2X_1$ cDNA (Genbank X80477), 1–994 in $rP2X_2$ cDNA (Genbank U14414), 1–673 in $rP2X_3$ cDNA (Genbank X90651), 1–670 in $rP2X_4$ cDNA (Genbank X91200), 1–1257 in $rP2X_5$ cDNA (Genbank X92069) and 1–581 in $rP2X_6$ cDNA (Genbank X92070).

In situ hybridization was carried out using a method modified from Höefler *et al*. (1986). Briefly, ganglia sections which had been treated as described above were washed in 0.1 M glycine/PBS and in 0.4% Triton X-100/PBS for 10 min each. The sections were then incubated in protease K (1 μg ml^{-1}) in PBS (Sigma) for 30 min at 37°C. The activity of protease K was stopped by fixation in 4% paraformaldehyde for 5 min, followed by 2 × 3 min wash in PBS to remove the fixative from the sections. The sections were incubated in 0.25% acetic anhydride with 0.1 M triethanolamine (pH 8.0) for 10 min at room temperature, followed by washing in 2 × 0.6 M sodium chloride, 0.06 M sodium citrate (SSC) for 10 min. Digoxigenin-labelled cRNA (0.1–0.5 μg ml^{-1}) of either antisense or sense probes were added to hybridization buffer containing 50% formamide, 10% dextran sulphate, 0.3 M NaCl, 1 × Denhardt's solution, 0.05 M Tris-HCl (pH 8.0), 1 mM EDTA and 250 μg ml^{-1} *E. Coli* tRNA (RNase-free) (Sigma). Hybridization was carried out for 16 h at 63°C in a hybridization oven. The sections were washed in 4 × SSC for 20 min at 37°C, followed by incubation in 2 × SSC containing 20 μg ml^{-1} RNase A (Sigma) for 30 min at 37°C to digest the RNA probes that did not hybridize with the targeted RNA. The sections were further washed in 1 × SSC and 0.2 × SSC at 37°C for 20 min, respectively. A method modified from Kiyama & Emson (1990) was used to detect the hybridization signals. Briefly, the sections were first incubated in the blocking buffer containing 5% bovine serum albumin

and 0.4% Triton X-100 in PBS at room temperature for 30 min, and then with anti-digoxigenin antibody conjugated to alkaline phosphatase (Boehringer Mannheim) diluted 1 : 1000 in the blocking buffer for 4 h at room temperature. The sections were washed with PBS for 4×5 min, followed by washing in 0.1 M Tris-HCl buffer, pH 8.0, containing 0.1 M NaCl and 0.01 M $MgCl_2$, then equilibrated for 10 min in 0.1 M Tris-HCl buffer, pH 9.5, with 0.1 M NaCl and 0.05 M $MgCl_2$. The colour development was performed with 400 μg ml^{-1} nitro blue tetrazolium, 200 μg ml^{-1} 5-bromo-4-chloro-3-indolyl phosphate and 100 μg ml^{-1} levamisole in 0.1 M Tris-HCl buffer, pH 9.5, containing 0.1 M NaCl and 0.05 M $MgCl_2$, in the dark at room temperature overnight. The sections were rinsed in 10 mM Tris-HCl, 1 mM EDTA, pH 8.0, for 10 min to stop the colour development, then mounted with 50% glycerol in the Tris-HCl/EDTA buffer and stored at 4°C in the dark.

Immunohistochemistry Sequence analysis has revealed that the C-terminal region is one of the least conserved amongst members of the P2X receptor family. Peptide sequence in this region has been used to generate subtype-selective antibodies (Roche Bioscience). A synthetic peptide corresponding to the C-terminal 15 amino acid residues (458–472) of the rat $P2X_2$ receptor (QQDSTSTDPKGLAQL; Genbank U14414) was covalently linked to Keyhole Limpet Haemocyanin, and rabbits were immunized with the conjugated peptide in multiple monthly injection (performed by Research Genetics, Inc., Huntsville, AL, U.S.A.). The specificity of the antisera was verified by immunoblotting with the membrane preparation from CHO-K1 cells expressing the cloned $P2X_2$ receptor. IgG fractions were isolated from the pre-immune and immune sera following the method of Harboe & Ingild (1973). The protein concentration was determined at 280 nm using an extinction factor of 1.43 for 1 mg ml^{-1}.

Sections which had been treated as described above were incubated in 0.5% H_2O_2 and 50% methanol for 10 min to block the endogenous peroxidase. The sections were then pre-incubated in 10% normal horse serum (Life Technologies) in PBS containing 0.05% methiolate for 20 min, followed by incubation with the primary antibodies diluted to 2.5 μg ml^{-1} (determined as optimal by previous titrations) in 10% normal horse serum in PBS containing 0.05% methiolate overnight. Subsequently the sections were incubated with biotinylated donkey anti-rabbit IgG (Jackson ImmunoResearch, West Grove, PA, U.S.A.) diluted 1 : 500 in 1% normal horse serum in PBS containing 0.05% methiolate for 1 h, and then with ExtrAvidin-horseradish peroxidase (Sigma) diluted 1 : 1500 in PBS containing 0.05% methiolate for 1 h. All incubations were held at room temperature and separated by 3×5-min washes in PBS. Finally, freshly prepared colour reaction mixture containing 0.5% 3,3′-diaminobenzidine, 0.1 M sodium phosphate, 0.004% NH_4Cl, 0.2% glucose, 0.04% nickel ammonium sulphate and 0.1% glucose oxidase were applied to the sections for 5–10 min or until colour product appeared (Llewellyn-Smith *et al*., 1993). The sections were then washed, dehydrated and cleared in xylene, and embedded.

Drugs and materials

ATP, related nucleotides and other chemicals were obtained from Sigma Chemical Co. (Poole, U.K.), except for 2-methylthio-ATP (2MeSATP), which was from RBI-SEMAT, (U.K.). Suramin was a gift from Bayer plc (U.K.), and pyridoxalphosphate-6-azophenyl-2′,4′-disulphonic acid (PPADS) was from Tocris Cookson, U.K. Stock solutions (10 mM, 100 mM) of ATP and other drugs were prepared using deionized water and stored frozen. All drugs were then diluted in extracellular bathing solution. The $P2X_2$ polyclonal antisera was kindly supplied by Roche Bioscience, Palo Alto, U.S.A. We would like to thank Dr G. Buell of Glaxo-Wellcome Institute of Molecular Biology in Geneva, Switzerland, for providing the rat $P2X_1$, $P2X_5$ and $P2X_6$ cDNA; Dr T. Blake of University of California, U.S.A., for providing rat $P2X_2$ cDNA and Dr J. Wood of University College London, U.K., for providing rat $P2X_3$ cDNA.

Results

Responses to ATP

Rapid application of ATP (100 μM) on to isolated rat MPG neurons voltage clamped at −70 mV induced an inward current in 268/277 cells. However, the peak amplitudes of these responses varied greatly (Figure 1a). Only a small response (<0.33 nA) was seen in 57.8% cells (160/277) while the remaining 39.0% cells (108/277) gave moderate-to-large inward currents (0.33–5.3 nA), including 11 cells which gave very large responses (>2 nA). This was not due simply to the difference in cell size, since a similar large degree of variation was still observed after normalizing the responses with respect to membrane capacitance (data not shown). A similar variation in the amplitude of inward currents evoked by ATP has been reported previously in dorsal root ganglion neurons (Robertson *et al*., 1996), and presumably reflects variability in the number of receptors expressed in different cells. Despite the large variability in response, the amplitude distribution revealed a single, though highly skewed, population.

The response to ATP occurred very rapidly, with a large increase in membrane conductance (Figure 1b), consistent with the activation of P2X receptors. The responses to ATP desensitized slowly, with the current produced by 100 μM declining to 43.8 ± 1.7% of control at the end of a 30 s application ($n = 4$). The decay of the current fitted well to a single exponential curve with a time constant of 24.0 ± 3.4 s, $n = 5$.

Concentration-effect relationships of the agonists

The concentration-effect relationship of ATP is shown in Figure 2. Fitting the Hill equation to the data gave an EC_{50} of 58.9 μM (log $EC_{50} = -4.23 \pm 0.06$, $n = 6$), and a Hill coefficient of 1.24, assuming the same relative E_{max} of 1.55 (see Methods section and Figure 7b). 2-Methylthio-ATP (2MeSATP), adenosine 5′-*O*-(3-thiotriphosphate) (ATPγS) and 2′,3′-*O*-(4-benzoylbenzoyl)-ATP (BzATP) were also effective, with 2MeSATP and ATPγS being slightly less potent than ATP (EC_{50}s of 85.7 μM and 84.2 μM, respectively, assuming the same maximum response). BzATP was considerably less potent, and although a maximum response was not obtained, the shape of the concentration-effect relationship of BzATP suggests that it may be a partial agonist at this receptor.

α,β-Methylene ATP (α,β-MeATP), β,γ-methylene ATP (β,γ-MeATP), uridine 5′-triphosphate (UTP) and adenosine 5′-diphosphate (ADP) were all inactive at concentations up to 100 μM.

Effects of antagonists

Suramin The P2 receptor antagonist suramin, (Dunn & Blakeley, 1988), reversibly reduced responses to ATP. With a

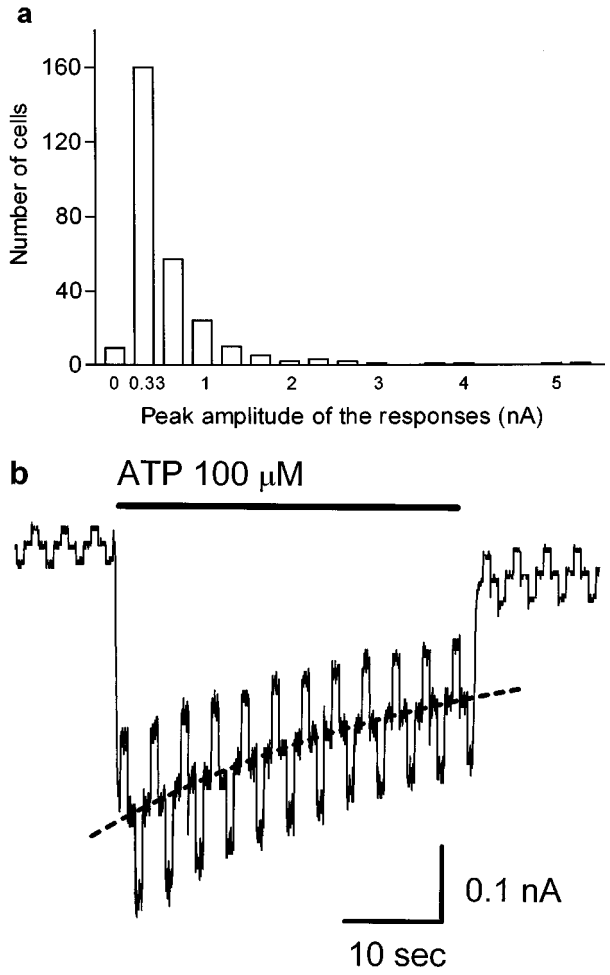

Figure 1 The inward currents induced by ATP on isolated rat major pelvic ganglia neurons. (a) The distribution of the peak amplitudes of the responses evoked by ATP (100 μM) in 277 cells. (b) Trace of the inward current activated by a prolonged application of ATP (100 μM). Membrane conductance was monitored by voltage commands ($\pm$10 mV, 750 ms) from a holding potential of $-$70 mV. The decline of the response was fitted to a single exponential curve (dashed line) to data points at $-$70 mV, with a time constant of 36 s.

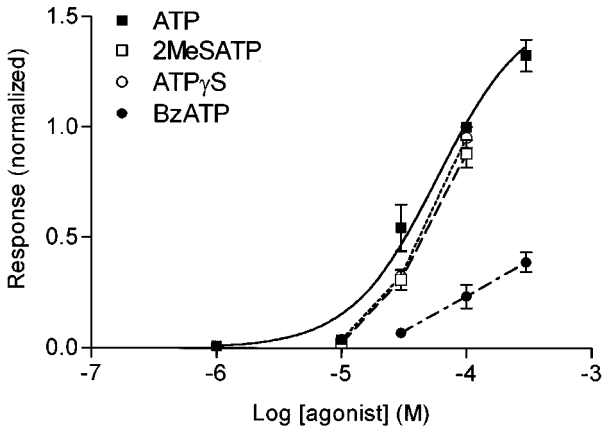

Figure 2 Concentration-effect curves for ATP, 2MeSATP, ATPγS and BzATP on rat major pelvic ganglia neurons. Cells were voltage clamped at $-$70 mV and various concentrations of agonists were applied for 5 s every 3 min. Each agonist was tested on a different sample of cells. The response to each agonist application was normalized with respect to that obtained with ATP (100 μM) on the same cell. Each point represents the mean$\pm$s.e.mean from four to six cells. The data for ATP were fitted with the Hill equation assuming relative maximum of 1.55 (see Methods), yielding an EC_{50} of 58.9 μM and a Hill coefficient of 1.24.

3 min pre-incubation, 100 μM suramin reduced responses to ATP (100 μM) to 2.7$\pm$1.7% of control (n=4). The responses recovered rapidly and were 69.8$\pm$7.2% (n=4) of control 3 min after washing out suramin. This antagonism produced by suramin appeared to be competitive, since the concentration-effect relationship for ATP was shifted to the right in an approximately parallel manner by 10 μM suramin (Figure 3a). Low concentrations of suramin (1 or 3 μM) have been found to produce approximately parallel, rightward shifts in the ATP concentration-response curves on heterologously expressed $P2X_1$ and $P2X_2$ receptors (Evans *et al*., 1995), but the shifts in the presence of higher concentrations were no longer parallel. Thus, the effect of suramin on P2X receptors may involve more than a competitive antagonism. Nevertheless, the antagonism by suramin (even at the higher concentration of 100 μM) was readily reversed within a few minutes of washout (e.g. Evans *et al*., 1995; this study). In the presence of suramin (10 μM) the concentration-effect relationship of ATP yielded an EC_{50} of 221 μM (log EC_{50} = $-$3.65$\pm$0.02, n=4, significantly different from control, P<0.0001, Student's t-test), and a Hill-slope of 1.88. Using a 2+2 type protocol, shifts in the concentration-response curves for ATP were determined for three concentrations of suramin. From these data, a Schild plot was constructed, which yielded a pA_2 of 5.5 with a slope of 0.63$\pm$0.10 (n=4) (Figure 3b).

Reactive blue-2 Another P2 receptor antagonist, reactive blue-2 (Cibacron Blue 3GA, 65% pure) (Manzini *et al*., 1986), was more effective than suramin in inhibiting responses to ATP. At 100 μM, reactive blue-2 was toxic to the MPG neurons (data not shown). Therefore, in this series of experiments, ATP was applied every 2 min. With a 2-min preincubation, 10 μM of reactive blue-2 was able to reduce responses to ATP (100 μM) to 2.5$\pm$1.4% of control (n=4), from which there was moderately rapid recovery of responses to 61.8$\pm$3.4% of control after a 2-min wash-out. However, the effect of reactive blue-2 did not appear to be competitive, since in the presence of 1 μM reactive blue-2, the E_{max} of the concentration-effect relationship of ATP was reduced (relative E_{max}=0.55$\pm$0.06, n=4, significantly different from control, P<0.001, Student's t-test, Figure 4a). Inhibition of the response to ATP (100 μM) by reactive blue-2 was concentration dependent (Figure 4b). Fitting the Hill equation to these data gave an IC_{50} of 0.7 μM (log IC_{50} = $-$6.15$\pm$0.10, n=6).

PPADS PPADS, another P2 receptor selective antagonist (Lambrecht *et al*., 1992), was also able to inhibit responses to ATP on MPG neurons. PPADS has two types of action on different recombinant P2X receptors. On $P2X_1$ and $P2X_2$, it shows slow onset of inhibition and slow recovery (up to 30 min) after washout, while on $P2X_3$, the onset of inhibition and recovery from PPADS is rapid (for review, see Buell *et al*., 1996a). On MPG neurons, its kinetics were considerably slower than those of suramin and reactive blue-2. After a 4 min pre-incubation, 10 μM PPADS reduced responses to ATP (100 μM) to 4.7$\pm$1.8% of control (n=4) (Figure 5a). The recovery from the inhibition of PPADS was also slow, with responses to ATP (100 μM) being only 20.5$\pm$1.7% of control (n=4) 4 min after washing out the antagonist. The time required for PPADS to inhibit responses of ATP was concentration-dependent. The time profile of the inhibition

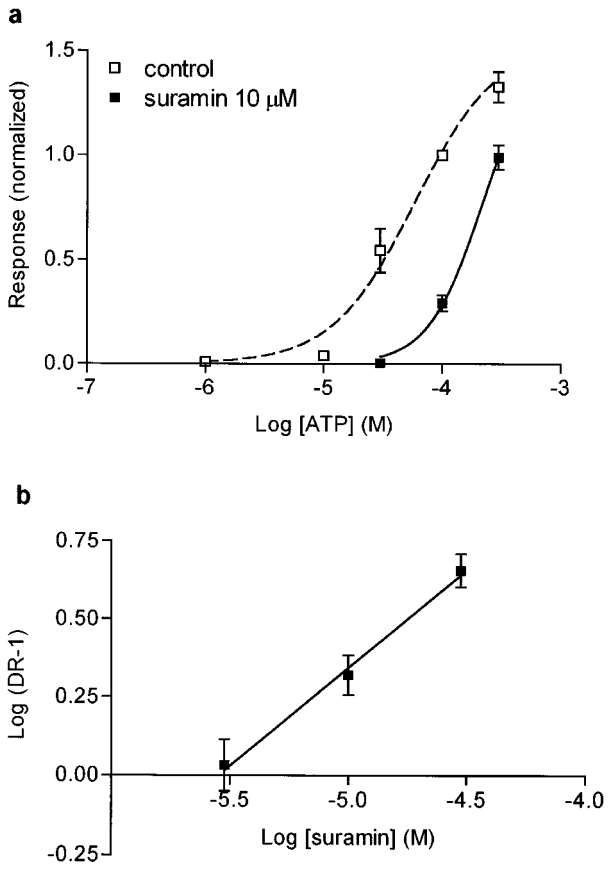

Figure 3 Effect of suramin on responses to ATP of rat major pelvic ganglia neurons. (a) Concentration-effect curves for ATP in the absence and presence of suramin (10 μM). Responses were normalized with respect to that obtained with ATP (100 μM) in the absence of suramin on the same cell. In the presence of suramin, the data for ATP were fitted with the Hill equation assuming relative maximum of 1.55 (see Methods), yielding an EC_{50} of 221 μM and a Hill coefficient of 1.88. Each point represents the mean $\pm$ s.e.mean from four cells. The concentration-effect curve for ATP in the absence of suramin (control) was taken from Figure 2. (b) Schild plot for the antagonism by suramin of responses to ATP, yielded a pA_2 of 5.5. DR = dose-ratio measured from the displacement of ATP dose-response lines by different concentrations of suramin. Each concentration of suramin was tested on a different sample of cells. Each data point represents the mean $\pm$ s.e.mean from four cells, from three to four separate experiments.

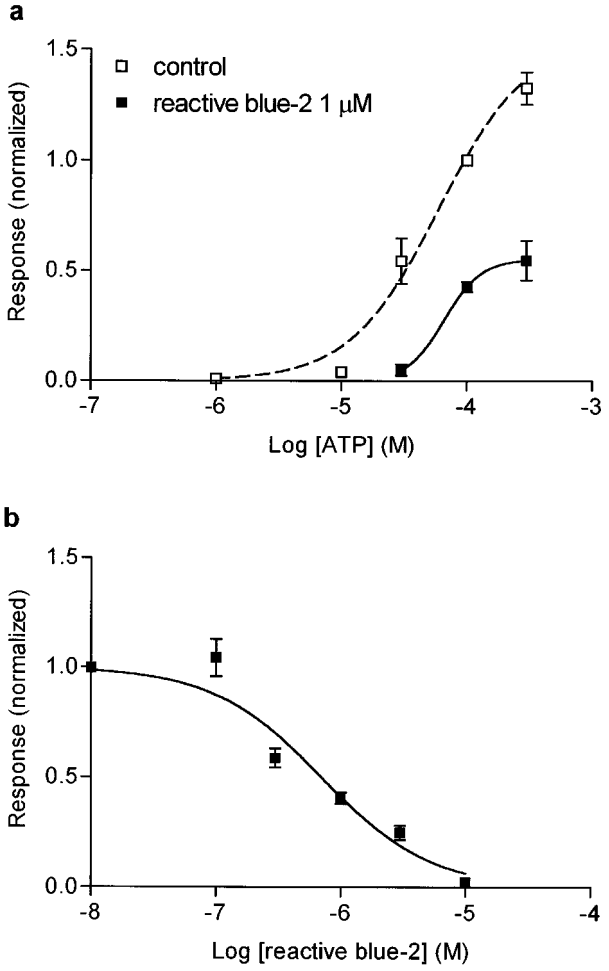

Figure 4 Effect of reactive blue-2 on responses to ATP of rat major pelvic ganglia (MPG) neurons. (a) Concentration-effect curves for ATP in the absence and presence of reactive blue-2 (1 μM). The concentration-effect curve for ATP in the presence of reactive blue-2 was fitted with the Hill equation, yielded a reduced E_{max} of 0.55 ± 0.06, $n = 4$. The control curve to ATP was taken from Figure 2. (b) Concentration-effect curve for the inhibition by reactive blue-2 of responses to ATP (100 μM) of rat MPG neurons. Responses were normalized with respect to that obtained with ATP (100 μM) in the absence of reactive blue-2 on the same cell. Various concentrations of reactive blue-2 were present 2 min before and during the re-application of ATP. The line was drawn according to the Hill equation, with an IC_{50} of 0.7 μM, $n = 6$.

by PPADS of responses to ATP is shown in Figure 5b. These data were well fitted by the single exponential decay, yielding time constants of 20.1 min, 7.6 min and 0.48 min for 0.3, 1 and 3 μM PPADS respectively (Figure 5b).

Modulation by pH

Application of external bath solution with pH from 6.8 to 8.0 in the absence of ATP did not activate detectable currents in these neurons (data not shown). However, altering pH produced dramatic changes in the responses to ATP. As shown in Figure 6a, the amplitude of the inward current induced by ATP (30 μM) was increased greatly when pH was reduced from 7.4 to 6.8, and was markedly attenuated when pH was elevated from 7.4 to 8.0. Proton potentiation of currents activated by ATP was rapid and reversible. On average, the current activated by ATP (30 μM) was enhanced at pH 6.8 to $339.2 \pm 28.4\%$ ($n = 4$) of that at pH 7.4 (control), while alkalinization to pH 8.0 suppressed the response to $20.2 \pm 3.0\%$ of control ($n = 4$) (Figure 6b).

The concentration-effect relationship for ATP-activated currents at pH 8.0, 7.4 and 6.8 showed that changing pH did not alter the slope of the concentration-effect relationship for ATP, but rather changed the EC_{50}s (Figure 6c), from 58.9 μM at pH 7.4 to 28.8 μM (log $EC_{50} = -4.54 \pm 0.04$, $n = 5$) and 264 μM (log $EC_{50} = -3.58 \pm 0.03$, $n = 5$) at pH 6.8 and 8.0 respectively (EC_{50}s at pH 6.8 and 8.0 were significantly different from that at pH 7.4, $P < 0.01$, $P < 0.0001$, Student's t-test, respectively).

Modulation by Zn^{2+}

Application of Zn^{2+} in the absence of ATP did not activate detectable currents in these neurons (data not shown). Co-application of ATP and Zn^{2+} (1–100 μM) produced a concentration dependent potentiation of responses to ATP. Fitting the Hill equation to the enhancement by Zn^{2+} of responses to ATP (30 μM) yielded an EC_{50} for Zn^{2+} of 9.55 μM (log $EC_{50} = -5.02 \pm 0.14$, $n = 6-10$) and an E_{max} of

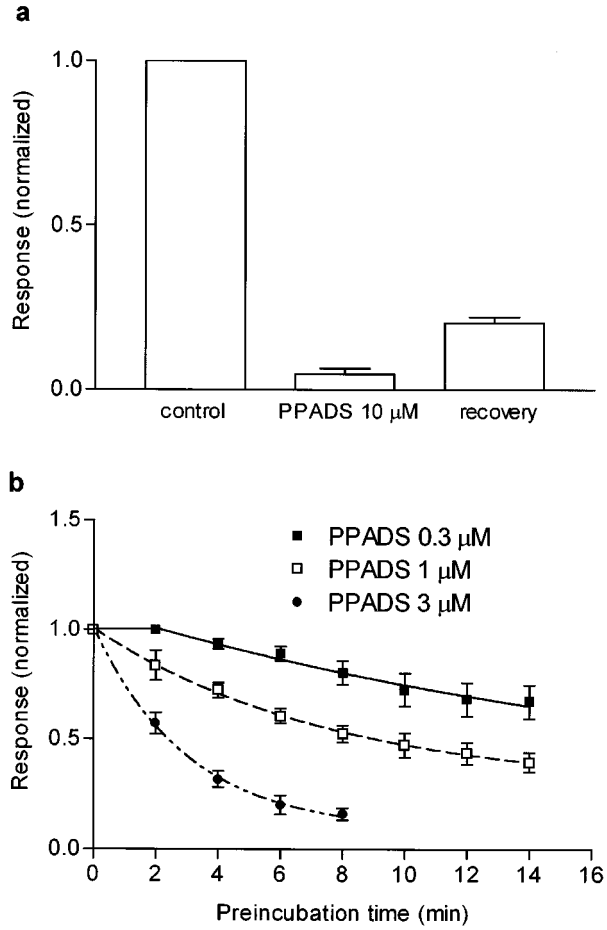

Figure 5 Effect of PPADS on responses to ATP of rat major pelvic ganglia neurons. (a) Histogram showing the peak amplitudes of the inward currents induced by ATP (100 μM) on its own, in the presence of PPADS (10 μM) and 4 min after washing-out PPADS. The antagonist was present 4 min before and during the re-application of ATP (100 μM). Each column represents the mean$\pm$s.e.mean from four cells. (b) Time profile of the inhibition by PPADS at concentrations of 0.3 μM, 1 μM and 3 μM. After determination of the control responses to ATP (100 μM), various concentrations of PPADS were applied to the cells, and ATP (100 μM) was reapplied every 2 min. Each concentration of PPADS was tested on a different sample of cells. Responses were normalized with respect to that obtained with ATP in the absence of PPADS on the same neuron. Data were fitted to the single exponential decay, yielding time constants of 20.1 min, 7.6 min and 0.48 min for 0.3, 1 and 3 μM PPADS, respectively, $n=4$. In the presence of 0.3 μM PPADS, curve fitting started from 2 min.

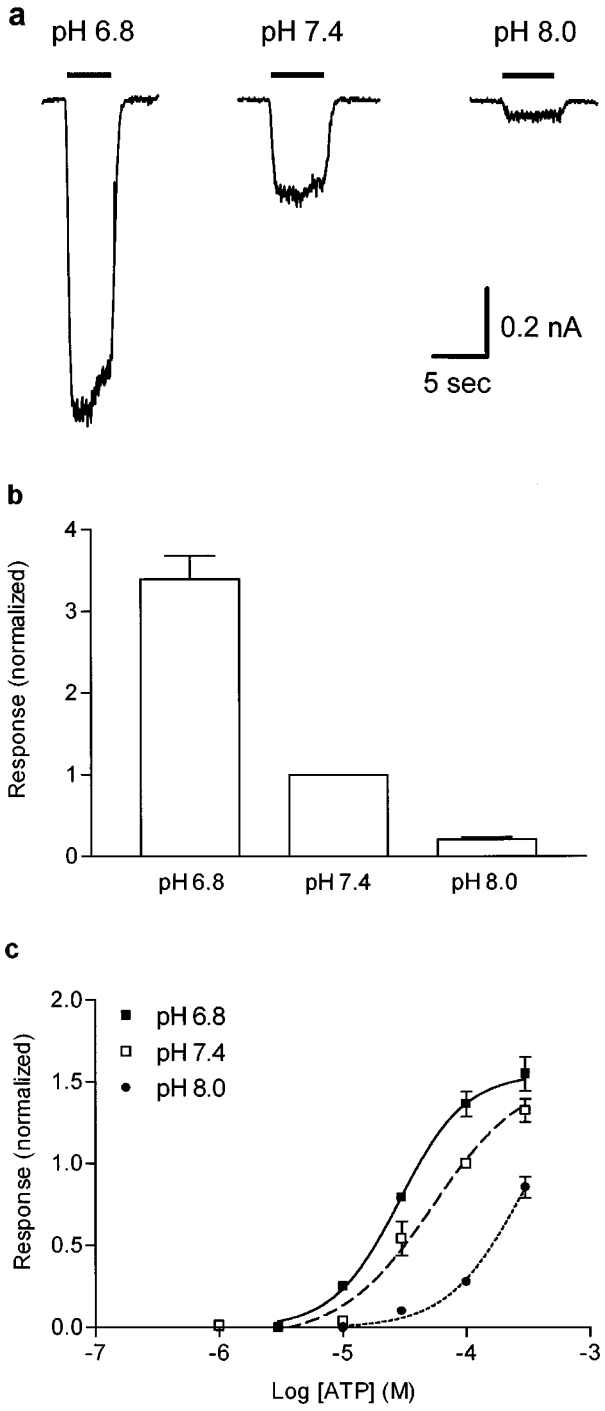

Figure 6 Effect of pH on ATP induced currents recorded from the rat major pelvic ganglia (MPG) neurons. (a) Traces showing responses to ATP (30 μM) of one rat MPG neuron at different pH. The horizontal bars represent the application time of ATP. (b) Averaged peak currents induced by ATP (30 μM) at pH 6.8, 7.4 and 8.0 from four cells. Currents were normalized in respect to that at pH 7.4 on the same cell. (c) Concentration-effect curves for ATP at pH 6.8, 7.4 and 8.0. Responses were normalized with respect to that evoked by ATP (100 μM) at pH 7.4 on the same cell. The control curve (pH 7.4) was taken from Figure 2. The data for ATP were fitted with the Hill equation assuming relative maximum of 1.55 (see Methods), yielding giving EC_{50}s of 28.8 and 264 μM at pH 6.8 and 8.0, respectively, $n=5$.

4.49 ± 0.48, with a Hill coefficient of 1.24 (Figure 7a). The concentration-effect relationships for ATP in the absence and presence of Zn^{2+} (30 μM) showed a parallel shift, with the EC_{50} of ATP decreasing to 4.57 μM (log $EC_{50}=-5.34\pm0.14$, $n=5$, significantly different from control, $P<0.0001$, Student's t-test) in the presence of Zn^{2+} (30 μM), while the Hill coefficient (1.19) and the E_{max} were not significantly altered (Figure 7b).

In situ *hybridization*

In situ hybridization using oligonucleotide probes specific for $P2X_{1-6}$ receptor mRNAs revealed marked difference in the levels of these transcripts in rat MPG neurons (Figure 8). $P2X_2$ receptor probe showed strong labelling in many neurons of MPG. However, there was considerable cell to cell variation in the intensity. $P2X_4$ receptor probe showed much less intense labelling. In contrast, the mRNA levels of $P2X_1$ and $P2X_3$ were hardly detectable. The mRNA levels of $P2X_5$ and $P2X_6$ receptors were also very low, similar to those of $P2X_1$ and $P2X_3$ (not shown).

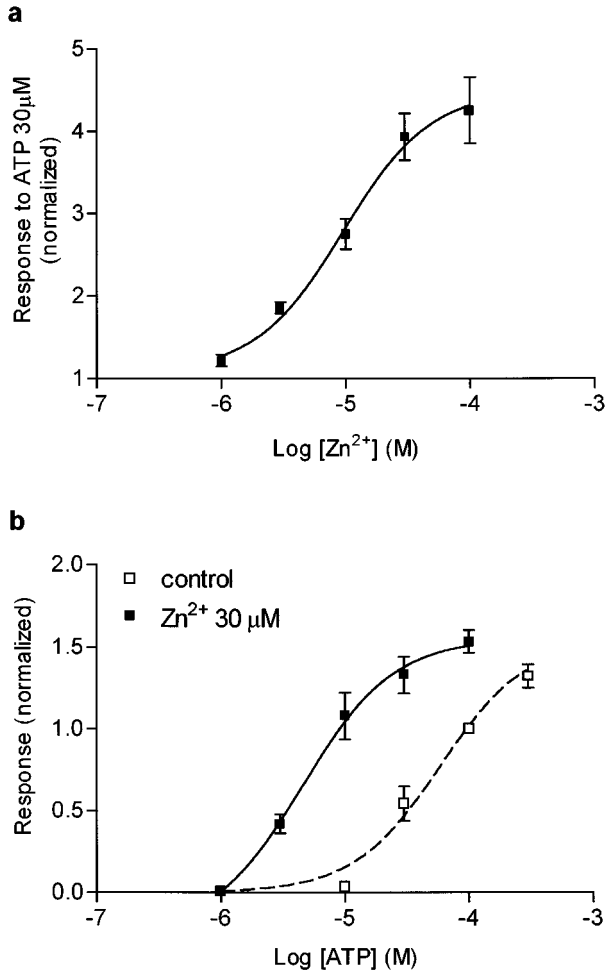

Figure 7 Effect of Zn^{2+} on ATP induced inward currents of the rat major pelvic ganglia (MPG) neurons. (a) Concentration-effect curve for the enhancement by Zn^{2+} of responses induced by ATP (30 μM) on rat MPG neurons. Responses were normalized with respect to that evoked by ATP (30 μM) in the absence of Zn^{2+} on the same cell. Fitting the Hill equation to the data yielded an EC_{50} of 9.55 μM, and a Hill coefficient of 1.24, $n=6-10$. (b) Concentration-effect curves for ATP in the absence and presence of Zn^{2+} (30 μM). Responses were normalized with respect to that induced by ATP (100 μM) in the absence of Zn^{2+} on the same cell. The control curve was taken from Figure 2. Data were fitted with the Hill equation without constraining the maximum, yielding an EC_{50} of 4.57 μM, a Hill coefficient of 1.19 and an E_{max} of 1.55 ± 0.12, $n=5$.

Immunohistochemistry

Since the *in situ* hybridization revealed a high level of $P2X_2$ receptor mRNA in many neurons of MPG, we examined this further by using immunohistochemical staining with the polyclonal antibody specific for $P2X_2$ receptor. The immunohistochemical staining revealed weaker staining on MPG compared with the nodose ganglia (Xiang, Z., Bo, X & Burnstock, G., personal communication). However, a small number of neurons showed specific and strong $P2X_2$ immunoreactivity (Figure 9).

Discussion

Our results clearly demonstrated for the first time, the presence of P2X receptors on rat MPG neurons (Figures 1, 8 and 9). However, there appears to be great variation in receptor density. Although many neurons contain a high level of $P2X_2$ receptor transcript, not all neurons show distinct $P2X_2$ labelling, with only a small percentage of neurons showing strong $P2X_2$ immunoreactivity. This is in agreement with our electrophysiological data, where out of 277 cells, only 11 cells give very large responses (>2 nA) to 100 μM ATP, while 57.8% cells produce only small responses (<0.33 nA). Thus, the large variation in the amplitude of inward currents evoked by ATP may reflect variability in the number of receptors expressed in different cells.

Pharmacological properties of these P2X receptors

Agonists On MPG neurons, ATP, 2MeSATP and ATPγS are full agonists (Figure 2), while α,β-MeATP and β,γ-MeATP are inactive. The lack of response to α,β-MeATP and β,γ-MeATP suggest that these purinoceptors are unlikely to be $P2X_1$ or $P2X_3$ subtypes (Valera *et al*., 1994; Chen *et al*., 1995). The EC_{50} value for ATP on MPG neurons is 58.9 μM, very similar to the value of 59.9 μM reported for $P2X_2$ subtype (Brake *et al*., 1994). Moreover, the responses to ATP desensitize slowly, with a $\tau=24$ s (Figure 1a), which would also be consistent with the characteristic of the $P2X_2$ subtype. The time constant for the decay of ATP responses on these neurons is longer than that determined for PC12 cells ($\tau=5.6$ s) (Nakazawa *et al*., 1990), but shorter than that for heterologously expressed $P2X_2$ ($\tau=57$ s) (Brändle *et al*., 1997).

Recently, a splice variant of the $P2X_2$ receptor has been identified. This $P2X_{2(b)}$ receptor desensitized four times more rapidly than the original $P2X_2$ (Simon *et al*., 1997; Brändle *et al*., 1997). However, the large difference in desensitization rate observed between these two studies makes comparison with our data inconclusive.

BzATP is ten times more potent than ATP as an agonist at the $P2X_7$ receptor (Surprenant *et al*., 1996), but acts as a weak partial agonist on MPG neurons. Although BzATP is also a partial agonist on heterologously expressed $P2X_1$ and $P2X_2$ receptors (Evans *et al*., 1995; King *et al*., 1996, 1997), it is 40 times more potent on the former ($EC_{50}=0.6$ μM, compared with 23 μM), and even more potent than on MPG neurons (EC_{50} estimated to be around 100 μM). The low potency of this agonist on MPG neurons would argue against the involvement of $P2X_7$ or $P2X_1$ receptors, but would again be consistent with the presence of $P2X_2$ receptors.

Antagonists

ATP responses on MPG neurons are antagonized by all three antagonists tested, suramin, reactive blue-2 and PPADS (Figures 3, 4 and 5). Reactive blue-2 and PPADS are more potent than suramin. The concentrations needed to achieve >95% inhibition of the response to ATP (100 μM) are 10 μM for reactive blue-2 and PPADS, and 100 μM for suramin. Suramin and reactive blue-2 have moderately fast onset and recovery, while it takes PPADS (<3 μM) 10 min or even longer to reach its maximal effect, and the recovery is also slow.

Currently available P2 receptor antagonists exhibit a limited ability to discriminate between subtypes. Since some $P2X_4$ receptors are insensitive to suramin, reactive blue-2 and PPADS, the sensitivity of the P2X receptors present on MPG neurons to antagonists would indicate that they are not the $P2X_4$ subtypes. However, it is difficult to rule out $P2X_4$ simply based on the sensitivity/insensitivity to antagonists. To date, several different $P2X_4$ subtypes have been cloned. While some are almost completely insensitive to suramin, PPADS and

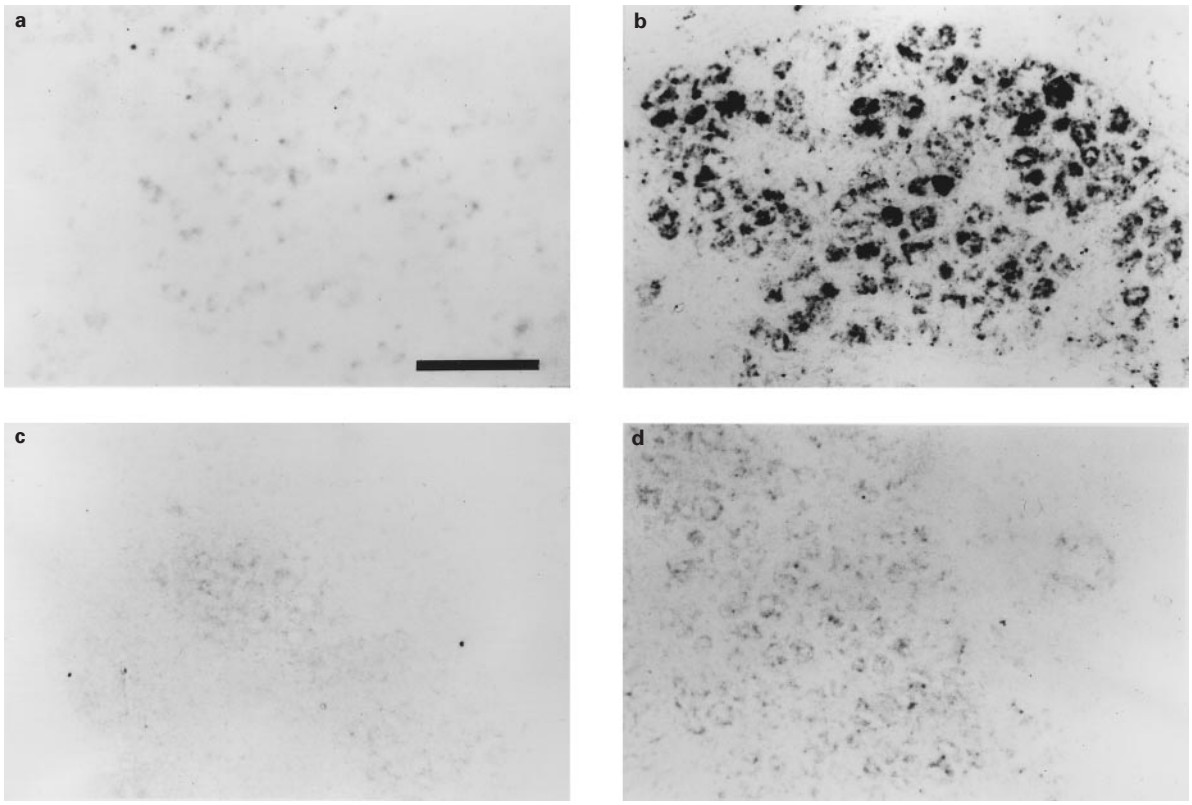

Figure 8 Detection of $P2X_{1-4}$ receptor mRNAs in the rat major pelvic ganglia using *in situ* hybridization with (a) $P2X_1$, (b) $P2X_2$, (c) $P2X_3$ and (d) $P2X_4$ oligonucleotide probes. Bar = 100 μm (a–d). Distinct labelling was observed with the $P2X_2$ probe, although there was great variation in the intensity from cell to cell. A much lower but still detectable level of staining was also seen with the $P2X_4$ probe.

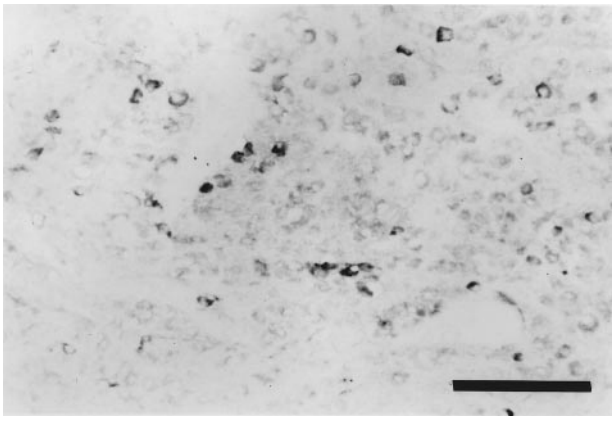

Figure 9 Immunohistochemical staining in the rat major pelvic ganglia using a polyclonal antibody specific for $P2X_2$ receptors. While the majority of neurons showed weak staining, a small percentage of neurons showed strong $P2X_2$-labelling. Bar = 200 μm.

reactive blue-2 (Bo *et al*., 1995; Buell *et al*., 1996b), others demonstrate small (Wang *et al*., 1996; Soto *et al*., 1996) to moderate sensitivity to these antagonists (Séguéla *et al*., 1996). Furthermore, the human $P2X_4$ receptors display a notably higher sensitivity to these antagonists than the rat homologue (Garcia-Guzman *et al*., 1997).

PPADS produces a slowly reversible antagonism at recombinant $P2X_1$, $P2X_2$ and $P2X_5$ receptors which has been attributed to the formation of a Schiff base with a specific lysine residue (Buell *et al*., 1996a). At other P2X receptors lacking this lysine, PPADS is a weak but rapidly reversible antagonist. Therefore, the slow kinetics for the action of PPADS on the P2X receptors present on MPG neurons would be consistent with the involvement of either $P2X_1$, $P2X_2$ and $P2X_5$ receptors.

Modulation by pH

Extracellular pH has very different effects on heterologously expressed $P2X_1$, $P2X_2$, $P2X_3$ and $P2X_4$ receptors (Stoop *et al*., 1997). The potency of ATP is decreased by acidification in cells expressing $P2X_1$, $P2X_3$ or $P2X_4$ receptors. However, at the $P2X_2$ receptor, acidification increases the potency of ATP. The recombinant $P2X_2$ receptor is so sensitive to the change in extracellular pH, that small acidic and alkaline shifts, as little as 0.03 pH-units, enhance or diminish the responses to ATP, respectively (King *et al*., 1996; Wildman *et al*., 1997). On MPG neurons, lowering the pH from 7.4 to 6.8 produces marked potentiation of the responses to ATP (30 μM), while raising the pH to 8.0 attenuates the responses (Figure 6). The affinity for ATP of these receptors is enhanced by acidification and decreased in an alkaline solution, which is consistent with the characteristic of the recombinant $P2X_2$ receptor.

Although the pH modulation observed is consistent with the presence of $P2X_2$ receptors, the heteromeric $P2X_{2/3}$ receptors also have a similar sensitivity to pH as homomeric $P2X_2$ receptors (Stoop *et al*., 1997). Presumably, the pH sensitivity on these heteromultimers is determined by the $P2X_2$ component. However, our *in situ* hybridization results would argue against involvement of the $P2X_{2/3}$ heteromer. Alternatively, as the $P2X_5$ receptor exhibits a remarkable similarity to the $P2X_2$ channel on its agonist profile and antagonist sensitivity (Garcia-Guzman *et al*., 1996), it is possible that the

change in extracellular pH might also have similar effects on $P2X_5$ and $P2X_2$ receptors. Therefore, although the pH sensitivity of ATP currents on MPG neurons is identical to that of the recombinant $P2X_2$ phenotype, the involvement of $P2X_5$ receptor can not be excluded.

Modulation by Zn^{2+}

Among the P2X receptor family, only $P2X_2$ and $P2X_4$ subtypes have been reported to be affected by Zn^{2+}. Simultaneous application of Zn^{2+} potentiates ATP-activated currents at the recombinant $P2X_2$ receptor (Brake *et al*., 1994; Wildman *et al*., 1998), as well as the $P2X_4$ receptor (Séguéla *et al*., 1996; Garcia-Guzman *et al*., 1997). ATP-activated currents are also potentiated by Zn^{2+} in rat sensory (nodose) (Li *et al*., 1993, 1996) and sympathetic (superior cervical ganglia) neurons (Cloues *et al*., 1993), by increasing the open frequency and burst duration of ATP-gated channels (Cloues, 1995; Wright & Li, 1995). The P2X receptors of rat sensory neurons are thought to be heteromultimeric assemblies of $P2X_2$ and $P2X_3$ subunits (Lewis *et al*., 1995), while rat sympathetic (superior cervical ganglia) neurons are known to contain $P2X_2$ transcripts (Collo *et al*., 1996). Thus, it seems likely that the presence of $P2X_2$ subunit confers the sensitivity of these native P2X receptors to Zn^{2+}.

On MPG neurons, ATP responses are strongly potentiated by Zn^{2+} (Figure 7). In this effect, Zn^{2+} has an EC_{50} of 9.6 μM, which is very close to that reported on recombinant $P2X_2$ receptor (Wildman *et al*., 1998). Thus, this feature of the P2X receptors on MPG neurons also shows the characteristics of $P2X_2$ subtype.

In situ *hybridization and immunohistochemical evidence*

While the pharmacological characteristics of these receptors are most consistent with them being the $P2X_2$ type, there is at present insufficient information on the $P2X_5$ receptor to rule it out pharmacologically. Using $P2X_{1-6}$ probes to hybridize with the MPG ganglion sections, only $P2X_2$ probe shows strong labelling, while $P2X_4$ probe gives some weak labelling and the mRNA levels for $P2X_1$, $P2X_3$, $P2X_5$ and $P2X_6$ are hard to detect. Since there appears to be a high level of $P2X_2$ receptor transcript in many neurons, we examined the level of $P2X_2$ receptor protein using an antisera specific for the $P2X_2$ receptor. While not all neurons show distinct $P2X_2$ labelling, there is a small percentage of neurons which show strong $P2X_2$ labelling. This great variability in receptor density strongly supports our electrophysiological data, which shows large variation in the peak amplitude of inward currents evoked by ATP. Furthermore, they also support the pharmacological data that $P2X_2$ is the major subtype of P2X receptors on these neurons.

In the central nervous system, $P2X_2$ mRNA has been localized in various brain regions using *in situ* hybridization (Kidd *et al*., 1995), while the $P2X_2$ receptor immunoreactivity has been reported in Purkinje cells, neurons in the granular and molecular layers and deep cerebellar nuclei in cerebellum (Kanjhan *et al*., 1996) and in several discrete populations of neurons, including those in the olfactory bulb, substantia nigra, ventral tegmental area and the locus coeruleus (Vulchanova *et al*., 1996). In the peripheral nervous system, $P2X_2$ RNA expression is detectable in nodose, superior cervical, coeliac and trigeminal ganglia (for review, see Buell *et al*., 1996a). In contrast to $P2X_2$, the expression pattern for $P2X_5$ is very restricted, and has only been detected in the trigeminal and dorsal root ganglia and the mesencephalic nucleus of the trigeminal nerve (Collo *et al*., 1996). Furthermore, cDNAs encoding three splice variants of the $P2X_2$ receptor, $P2X_{2(b)}$, $P2X_{2(c)}$ and $P2X_{2(d)}$, were isolated from rat cerebellum (Simon *et al*., 1997). Transcripts for $P2X_{2(b)}$ and $P2X_{2(c)}$ were present in many structures in the neonatal rat brain and in nodose, dorsal root and superior cervical ganglia. It remains to be seen whether any of these variants are also present on MPG.

Coexpression of more than one receptor subunit?

The coexpression of $P2X_2$ and $P2X_3$ receptor subunits are required to produce ATP-gated currents with the properties seen in some sensory neurons (Lewis *et al*., 1995). The P2X receptors present on guinea-pig myenteric neurons share some properties with the $P2X_4$ and $P2X_6$ receptors. The unusual pharmacological properties might result from the formation of heteromeric receptors from subunits with different functional properties (Barajas-López *et al*., 1996). In another study, Zhou & Galligan (1996) demonstrated that there are more than one type of P2X receptors on myenteric neurons, one having the properties similar to cloned $P2X_1$ receptors, and another more like cloned $P2X_2$ or $P2X_5$ receptors. The P2X receptors in superior cervical ganglion neurons may represent $P2X_2$ or $P2X_5$ subtypes, different from those present in nodose and coeliac neurons (Khakh *et al*., 1995). In parasympathetic cardiac ganglion neurons, the characteristics of those purinoceptors suggest that they are also heteromultimeric (Fieber & Adams, 1991).

Our study demonstrates that on pelvic ganglia, unique within the autonomic nervous system because they contain both sympathetic and parasympathetic neurons, there exist P2X receptors similar to those on superior cervical ganglia, and apparently of the $P2X_2$ subtype. However, in light of the evidence obtained from our *in situ* hybridization study, where although neurons of the MPG show high levels of $P2X_2$ receptor transcript they also possess a much lower but clearly detectable level of $P2X_4$ mRNA, it is possible that the P2X receptors on MPG are heteromultimers, with $P2X_2$ being the dominant component. Alternative splicing of pre-mRNA is a common phenomenon for other transmitter-gated channels. The recently identified splice variants of $P2X_2$ receptor (Simon *et al*., 1997) may increase the number of subunit sequences available for heteromultimeric channel assembly.

Which neurons in MPG express P2X receptors?

As mentioned previously, pelvic ganglia contain a mixture of sympathetic and parasympathetic neurons which are innervated by preganglionic axons from either hypogastric nerve (sympathetic) or pelvic nerve (parasympathetic), respectively. These two types of neurons are present in approximately equal proportions (Keast, 1995). Of those neurons receiving sympathetic preganglionic innervation, the majority ($\sim$75%) of them are noradrenergic (i.e. immunoreactive for tyrosine hydroxylase (TH)), and are also immunoreactive for neuropeptide Y (NPY); the remainder contain vasoactive intestinal peptide (VIP)-immunoreactivity (IR) but not TH-IR and maybe cholinergic. Those neurons receiving parasympathetic preganglionic innervation are virtually all non-noradrenergic (no TH-IR) and are also of two histochemical types, with some neurons containing NPY-IR and others containing VIP-IR (Keast, 1995). Furthermore, by using the retrograde-tracing technique, the peptide contents of MPG neurons that project to different urogenital organs and digestive tracts have been identified (Keast & de Groat, 1989; Luckensmeyer & Keast,

1995). The results from our study indicated that the density of P2X receptors on the ganglia and the responses to ATP vary widely from cell to cell (Figures 1, 8 and 9), and the amplitude distribution indicates a single but highly skewed population (Figure 1). It remains to be seen whether there is a correlation between the neuron type, their peptide contents and/or their projection to various pelvic organs with the level of P2X receptor expression.

To conclude, we have demonstrated the presence of P2X receptors on rat major pelvic ganglia neurons. The pharmacological characteristics of these receptors, the *in situ* hybridization and immunohistochemical evidence are all consistent with them being of the $P2X_2$ subtype, or heteromultimers with $P2X_2$ being the dominant component.

The authors are grateful to Prof Ute Gröschel-Stewart for help and advice regarding immunohistochemical methods, to E.W. Moules and T.P. Robson for the excellent technical support, to Mr R. Jordan for the help in the preparation of the manuscript and to Dr B. King and Dr A. Townsend-Nicholson for helpful discussion. This work was supported by Roche Bioscience and the British Heart Foundation.

References

ABBRACCHIO, M.P. & BURNSTOCK, G. (1994). Purinoceptors: are there families of P2X and P2Y purinoceptors? *Pharmacol. Ther.,* **64,** 445 – 475.

ARUNLAKSHANA, O. & SCHILD, H.O. (1959). Some quantitative uses of drug antagonists. *Br. J. Pharmacol.,* **14,** 151 – 161.

BARAJAS-LÓPEZ, C., HUIZINGA, J.D., COLLINS, S.M., GERZANICH, V., ESPINOSA-LUNA, R. & PERES, A.L. (1996). P2X-purinoceptors of myenteric neurones from the guinea-pig ileum and their unusual pharmacological properties. *Br. J. Pharmacol.,* **119,** 1541 – 1548.

BEAN, B.P. (1990). ATP-activated channels in rat and bullfrog sensory neurons: concentration dependence and kinetics. *J. Neurosci.,* **10,** 1 – 10.

BO, X., ZHANG, Y., NASSAR, M., BURNSTOCK, G. & SCHOEPFER, R. (1995). A P2X purinoceptor cDNA conferring a novel pharmacological profile. *FEBS Lett.,* **375,** 129 – 133.

BRAKE, A.J., WAGENBACH, M.J. & JULIUS, D. (1994). New structural motif for ligand-gated ion channels defined by an ionotropic ATP receptor. *Nature,* **371,** 519 – 523.

BRÄNDLE, U., SPIELMANNS, P., OSTEROTH, R., SIM, J., SURPRENANT, A., BUELL, G., RUPPERSBERG, J.P., PLINKERT, P.K., ZENNER, H.-P. & GLOWATZKI, E. (1997). Desensitization of the $P2X_2$ receptor controlled by alternative splicing. *FEBS Lett.,* **404,** 294 – 298.

BUELL, G., COLLO, G. & RASSENDREN, F. (1996a). P2X receptors: an emerging channel family. *Eur. J. Neurosci.,* **8,** 2221 – 2228.

BUELL, G., LEWIS, C., COLLO, G., NORTH, R.A. & SURPRENANT, A. (1996b). An antagonist-insensitive P2X receptor expressed in epithelia and brain. *EMBO J.,* **15,** 55 – 62.

CHEN, C.-C., AKOPIAN, A.N., SIVILOTTI, L., COLQUHOUN, D., BURNSTOCK, G. & WOOD, J.N. (1995). A P2X purinoceptor expressed by a subset of sensory neurons. *Nature,* **377,** 428 – 431.

CLOUES, R. (1995). Properties of ATP-gated channels recorded from rat sympathetic neurons: voltage dependence and regulation by Zn^{2+} ions. *J. Neurophysiol.,* **73,** 312 – 319.

CLOUES, R., JONES, S. & BROWN, D.A. (1993). Zn^{2+} potentiates ATP-activated currents in rat sympathetic neurons. *Pflugers Arch.,* **424,** 152 – 158.

COLLO, G., NORTH, R.A., KAWASHIMA, E., MERLO-PICH, E., NEIDHART, S., SURPRENANT, A. & BUELL, G. (1996). Cloning of $P2X_5$ and $P2X_6$ receptors and the distribution and properties of an extended family of ATP-gated ion channels. *J. Neurosci.,* **16,** 2495 – 2507.

DUNN, P.M. & BLAKELEY, A.G.H. (1988). Suramin: a reversible P2-purinoceptor antagonist in the mouse vas deferens. *Br. J. Pharmacol.,* **93,** 243 – 245.

DUNN, P.M., BENTON, D.C., CAMPOS-ROSA, J., GANELLIN, C.R. & JENKINSON, D.H. (1996). Discrimination between subtypes of apamin-sensitive Ca^{2+}-activated K^+ channels by gallamine and a novel bis-quaternary quinolinium cyclophane, UCL 1530. *Br. J. Pharmacol.,* **117,** 35 – 42.

EDWARDS, F.A., GIBB, A.J. & COLQUHOUN, D. (1992). ATP receptor-mediated synaptic currents in the central nervous system. *Nature,* **359,** 144 – 147.

EVANS, R.J., LEWIS, C., BUELL, G., VALERA, S., NORTH, R.A. & SURPRENANT, A. (1995). Pharmacological characterization of heterologously expressed ATP-gated cation channels (P2X purinoceptors). *Mol. Pharmacol.,* **48,** 178 – 183.

FIEBER, L.A. & ADAMS, D. (1991). Adenosine triphosphate-evoked currents in cultured neurones dissociated from rat parasympathetic cardiac ganglia. *J. Physiol.,* **434,** 239 – 256.

GARCIA-GUZMAN, M., SOTO, F., LAUBE, B. & STÜHMER, W. (1996). Molecular cloning and functional expression of a novel rat heart P2X purinoceptor. *FEBS Lett.,* **388,** 123 – 127.

GARCIA-GUZMAN, M., SOTO, F., GOMEZ-HERNANDEZ, J.M., LUND, P. & STÜHMER, W. (1997). Characterization of recombinant human $P2X_4$ receptor reveals pharmacological differences to the rat homologue. *Mol. Pharmacol.,* **51,** 109 – 118.

HARBOE, N. & INGILD, A. (1973). Immunization, isolation of immunoglobulins, estimation of antibody titre. *Scand. J. Immunol. Suppl.,* **1,** 161 – 164.

HÖEFLER, H., CHILDERS, H., MONTMINY, M.R., LECHAN, R.M., GOODMAN, R.H. & WOLFE, H.J. (1986). In situ hybridization methods for the detection of somatostatin mRNA in tissue sections using antisense RNA probes. *Histochem. J.,* **18,** 597 – 604.

KANJHAN, R., HOUSLEY, G.D., THORNE, P.R., CHRISTIE, D.L., PALMER, D.J., LUO, L. & RYAN, A. (1996). Localization of ATP-gated ion channels in cerebellum using $P2X_2R$ subunit-specific antisera. *NeuroReport,* **7,** 2665 – 2669.

KEAST, J.R. (1995). Visualization and immunohistochemical characterization of sympathetic and parasympathetic neurons in the male rat major pelvic ganglion. *Neuroscience,* **66,** 655 – 662.

KEAST, J.R. & DE GROAT, W.C. (1989). Immunohistochemical characterization of pelvic neurons which project to the bladder, colon, or penis in rats. *J. Comp. Neurol.,* **288,** 387 – 400.

KHAKH, B.S., HUMPHREY, P.P.A. & SURPRENANT, A. (1995). Electrophysiological properties of P2X-purinoceptors in rat superior cervical, nodose and guinea-pig coeliac neurones. *J. Physiol.,* **484,** 385 – 395.

KIDD, E.J., GRAHAMES, C.B.A., SIMON, J., MICHEL, A.D., BARNARD, E.A. & HUMPHREY, P.P.A. (1995). Localization of P2X purinoceptor transcripts in the rat nervous system. *Mol. Pharmacol.,* **48,** 569 – 573.

KING, B.F., ZIGANSHINA, L.E., PINTOR, J. & BURNSTOCK, G. (1996). Full sensitivity of $P2X_2$ purinoceptor to ATP revealed by changing extracellular pH. *Br. J. Pharmacol.,* **117,** 1371 – 1373.

KING, B.F., WILDMAN, S.S., ZIGANSHINA, L.E., PINTOR, J. & BURNSTOCK, G. (1997). Effects of extracellular pH on agonism and antagonism at a recombinant $P2X_2$ receptor. *Br. J. Pharmacol.,* **121,** 1445 – 1453.

KIYAMA, H. & EMSON, P.C. (1990). Distribution of somatostatin mRNA in the rat nervous system as visualized by a novel non-radioactive in situ hybridization histochemistry procedure. *Neuroscience,* **38,** 223 – 244.

KRISHTAL, O.A. & PIDOPLICHKO, V.I. (1980). A receptor for protons in the nerve cell membrane. *Neuroscience,* **5,** 2325 – 2327.

KRISHTAL, O.A., MARCHENKO, S.M. & PIDOPLICHKO, V.I. (1983). Receptor for ATP in the membrane of mammalian sensory neurones. *Neurosci. Lett.,* **35,** 41 – 45.

KRISHTAL, O.A., MARCHENKO, S.M., OBUKHOV, A. & VOLKOVA, T.M. (1988). Receptors for ATP in rat sensory neurones: the structure-function relationship for ligands. *Br. J. Pharmacol.,* **95,** 1057 – 1062.

LAMBRECHT, G., FRIEBE, T., GRIMM, U., WINDSCHEIF, U., BUNGARDT, E., HILDEBRANDT, C., BÄUMERT, H.G., SPATZ-KÜMBEL, G. & MUTSCHLER, E. (1992). PPADS, a novel functionally selective antagonist of P2 purinoceptor-mediated responses. *Eur. J. Pharmacol.,* **217,** 217 – 219.

LANGWORTHY, O.R. (1965). Innervation of the pelvic organs of the rat. *Invest. Urol.,* **2,** 491 – 511.

LEWIS, C., NEIDHART, S., HOLY, C., NORTH, R.A., BUELL, G. & SURPRENANT, A. (1995). Coexpression of $P2X_2$ and $P2X_3$ receptor subunits can account for ATP-gated currents in sensory neurons. *Nature,* **377,** 432–435.

LI, C., PEOPLES, R.W., LI, Z. & WEIGHT, F.F. (1993). Zn^{2+} potentiates excitatory action of ATP on mammalian neurons. *Proc. Natl. Acad. Sci. U.S.A.,* **90,** 8264–8267.

LI, C., PEOPLES, R.W. & WEIGHT, F.F. (1996). Proton potentiation of ATP-gated ion channel responses to ATP and Zn^{2+} in rat nodose ganglion neurons. *J. Neurophysiol.,* **76,** 3048–3058.

LLEWELLYN-SMITH, I.J., PILOWSKY, P. & MINSON, J.B. (1993). The tungstate-stabilized tetramethylbenzidine reaction for light and electron microscopic immunocytochemistry and for revealing biocytin-filled neurons. *J. Neurosci. Methods,* **46,** 27–40.

LUCKENSMEYER, G.B. & KEAST, J.R. (1995). Immunohistochemical characterization of sympathetic and parasympathetic pelvic neurons projecting to the distal colon in the male rat. *Cell Tissue Res.,* **281,** 551–559.

MANZINI, S., HOYLE, C.H.V. & BURNSTOCK, G. (1986). An electrophiological analysis of the effect of reactive blue-2, a putative P2-purinoceptor antagonist, on inhibitory junction potentials of rat caecum. *Eur. J. Pharmacol.,* **127,** 197–204.

NAKAZAWA, K., FUJIMORI, K., TAKANAKA, A. & INOUE, K. (1990). An ATP-activated conductance in pheochromocytoma cell and its suppression by extracellular calcium. *J. Physiol.,* **428,** 257–272.

NISHIMURA, T. & TOKIMASA, T. (1996). Purinergic cation channels in neurons of rabbit vesical parasympathetic ganglia. *Neurosci. Lett.,* **212,** 215–217.

PURINTON, P.T., FLETCHER, T.F. & BRADLEY, W.E. (1973). Gross and light microscopic features of the pelvic plexus in the rat. *Anat. Rec.,* **175,** 697–706.

ROBERTSON, S.J., RAE, M.G., ROWAN, E.G. & KENNEDY, C. (1996). Characterization of a P2X-purinoceptor in cultured neurones of the rat dorsal root ganglia. *Br. J. Pharmacol.,* **118,** 951–956.

SÉGUÉLA, P., HAGHIGHI, A., SOGHOMONIAN, J. & COOPER, E. (1996). A novel neuronal P2X ATP receptor ion channel with widespread distribution in the brain. *J. Neurosci.,* **16,** 448–455.

SIMON, J., KIDD, E.J., SMITH, F.M., CHESSELL, I.P., MURRELL-LAGNADO, R., HUMPHREY, P.P.A. & BARNARD, E.A. (1997). Localization and functional expression of splice variants of the $P2X_2$ receptor. *Mol. Pharmacol.,* **52,** 237–248.

SOTO, F., GARCIA-GUZMAN, GOMEZ-HERNANDEZ, J.M., HOLLMANN, M., KARSCHIN, C. & STÜHMER, W. (1996). $P2X_4$: an ATP-activated ionotropic receptor cloned from rat brain. *Proc. Natl. Acad. Sci. U.S.A.,* **93,** 3684–3688.

STOOP, R., SURPRENANT, A. & NORTH, R.A. (1997). Different sensitivities to pH of ATP-induced currents at four cloned P2X receptors. *J. Neurophysiol.,* **78,** 1837–1840.

SURPRENANT, A., RASSENDREN, F., KAWASHIMA, E., NORTH, R.A. & BUELL, G. (1996). The cytolytic P_{2Z} receptor for extracellular ATP identified as a P2X receptor ($P2X_7$). *Science,* **272,** 735–738.

VALERA, S., HUSSY, N., EVANS, R.J., ADAMI, N., NORTH, R.A., SURPRENANT, A. & BUELL, G. (1994). A new class of ligand-gated ion channel defined by P2X receptor for extracellular ATP. *Nature,* **371,** 516–519.

VULCHANOVA, L., ARVIDSSON, U., RIEDL, M., WANG, J., BUELL, G., SURPRENANT, A., NORTH, R.A. & ELDE, R. (1996). Differential distribution of two ATP-gated ion channels (P2X receptors) determined by immunocytochemistry. *Proc. Natl. Acad. Sci. U.S.A.,* **93,** 8063–8067.

WANG, C.-Z., NAMBA, N., GONOI, T., INAGAKI, N. & SEINO, S. (1996). Cloning and pharmacological characterization of a fourth P2X receptor subtype widely expressed in brain and peripheral tissues including various endocrine tissues. *Biochem. Biophysic. Res. Commun.,* **220,** 196–202.

WILDMAN, S.S., KING, B.F. & BURNSTOCK, G. (1997). Potentiation of ATP-responses at a recombinant $P2X_2$ receptor by neurotransmitters and related substances. *Br. J. Pharmacol.,* **120,** 221–224.

WILDMAN, S.S., KING, B.F. & BURNSTOCK, G. (1988). Zn^{2+} modulation of ATP-responses at recombinant $P2X_2$ receptors and its dependence on extracellular pH. *Br. J. Pharmacol.,* **123,** 1214–1220.

WRIGHT, J.M. & LI, C. (1995). Zn^{2+} potentiates steady-state ATP activated currents in rat nodose ganglion neurons by increasing the burst duration of a 35 pS channel. *Neurosci. Lett.,* **193,** 177–180.

ZHOU, X. & GALLIGAN, J.J. (1996). P2X purinoceptors in cultured myenteric neurons of guinea-pig small intestine. *J. Physiol.,* **496,** 719–729.

(Received June 20, 1998
Revised July 15, 1998
Accepted July 16, 1998)